

Ex-vivo Evaluation of Newly Formed Bone After Lumbar Interbody Fusion Surgery Using X-ray Micro Computed Tomography



Jakub Laznovsky , Adam Brinek , Tomas Zikmund ,
and Jozef Kaiser 

Abstract Many novel biomaterials are recently investigated for use in spinal fusion surgery, especially in lumbar interbody fusion. The X-ray microCT as a tool is widely used for evaluating how successfully those biomaterials can perform a vertebral fusion. However, the current methodologies of microCT image assessment are based on visual evaluation by the operator. In this paper, we propose a methodology for how such biomaterials can be investigated in pre-clinical studies by investigating fused vertebrae morphology. We utilized microCT scans of pigs' fused vertebrae to develop a fully automatic approach, which can characterize the morphometry of the bone in the fused region. A surface mesh model was created to extract the newly formed bone tissue between fused vertebrae in the microCT data. Extracted bone tissue was consequently evaluated according to the selected morphometric parameters. Characterization of the newly formed bone properties in the intervertebral area can be utilized to evaluate the osteogenesis function of implants used in lumbar interbody fusion surgery.

Keywords X-ray micro computed tomography · Intervertebral fusion · Image processing · Lumbar interbody fusion · Quantitative tomography

J. Laznovsky (✉) · A. Brinek · T. Zikmund · J. Kaiser
CEITEC-Central European Institute of Technology, Brno University of Technology, 612 00 Brno,
Czech Republic
e-mail: Jakub.Laznovsky@ceitec.vutbr.cz

A. Brinek
e-mail: Adam.Brinek@ceitec.vutbr.cz

T. Zikmund
e-mail: Tomas.Zikmund@ceitec.vutbr.cz

J. Kaiser
e-mail: Jozef.Kaiser@ceitec.vutbr.cz

1 Introduction

Spinal fusion is a neurosurgical technique that connects two or more vertebrae to prevent a motion between them. This technique is performed for the treatment of various degenerative diseases to relieve back pain and pressure. Since the early 1900s, bone grafts have been used as a source of growth factors to reach a permanent vertebral fusion. The bone graft (autograft) is surgically removed from another part of the patient body, usually from the iliac crest. This method remains a standard up to recent times. Currently, the huge expanse of biomaterials used in medicine brings many new approaches to spinal fusion every year [1–4]. Usage of biomaterials is beneficial in this case due to the possibility of fusion rate regulation and complicated obtaining of the autografts. Evaluation of the vertebral fusion quality in order to evaluate individual biomaterials is therefore fundamental.

Micro Computed Tomography (microCT) plays an important role in the fusion quality assessment. Thanks to the 3D non-destructive visualization and quantitative analysis of Lumbar Interbody Fusion (LIF) location, it is possible to evaluate bone tissue properties. According to previous studies, the accuracy of microCT for bone morphometry is closely correlated with histomorphometric techniques [5–7]. In the case studies, which can proceed *ex-vivo*, the advantage of microCT can be taken. The main benefit of microCT compared to a clinical CT scanner is the spatial resolution of the scan in order of micrometers (dependent on the size of the sample).

In the case of LIF quality assessment using microCT, it is crucial to select an objective and standardized approach for the LIF area analysis. Several automated approaches for the LIF area were already introduced but usually require some enhancement or are suitable for a method other than microCT, especially for clinical applications (plain radiography, clinical CT, magnetic resonance imaging) [8–11]. Another category is visual methods, which are established but depend on the subjective evaluation by the operator [12, 13]. The development of a standardized approach can facilitate the comparison of the vertebral samples, where vertebrae are fused with different types of intervertebral implants, including bone grafts.

In this work, we extended analyses from [14] and analyzed the vertebral samples after LIF in detail using quantitative parameters evaluating the newly formed bone properties. The main motivation is to provide a tool which can easily and objectively analyze LIF area structure, using different biomaterials used for vertebral fusion. Such a methodology can consequently facilitate and accelerate the investigation of biomaterials suitable for vertebral fusion. Automation of this process is crucial, since manual methods are affected by bias caused by the operator.

2 MicroCT Bone Tissue Evaluation

The formation of new bone after LIF surgery is possible thanks to the osteogenic, osteoinductive, and osteoconductive properties of fusion materials used for vertebral fusion [15]. Since bone fusion is artificially created, the properties of the newly formed bone tissue may vary from individual to individual. Bone morphometry is able to quantitatively describe the correlation between the growth and development of the examined bone and the type of material used for spinal fusion.

Besides, microCT is capable to evaluate bone samples to study metabolic bone diseases such as osteoporosis and characterize the efficiency of therapies for these degenerative diseases [16]. The main benefit is the non-destructive evaluation of bone fragility, microdamages, and density. Consequently, it is possible to create 3D models of examined bones (vertebrae) for simulations of mechanical stress, and bone fragility induced by loading [17].

There are several morphological parameters that characterize the bone and can be derived directly from the microCT 3D image stack. These parameters are obtained by image-processing methods using various software provided by microCT manufacturers or by applying mathematical methods in a programming environment. There are four basic parameters characterizing the trabecular bone: Trabecular thickness (Tb.Th), separation (Tb.Sp), number (Tb.N), and bone volume fraction (BV/TV) [18]. Mean Tb.Th and Tb.Sp are evaluated using the sphere fitting method, where in the case of Tb.Th the biggest spheres inscribed in the individual parts of the segmented object are considered. In the case of Tb.Sp is the approach similar, but spheres are fitted into the gaps between trabeculae (image background). Individually fitted sphere diameters are consequently averaged to obtain a single representative Tb.Th or Tb.Sp value. BV/TV is based on the ratio of voxels belonging to the bone and to the volume of interest (VOI), and Tb.N can be derived as the proportion of BV/TV and Tb.Th.

Further parameters evaluating trabecular bone are Connectivity Density (Conn.D) and Degree of Anisotropy (DA). Connectivity is designed to estimate the number of connected trabeculae in a trabecular network. The calculation of connectivity is based on the Euler characteristics, which count the number of objects in VOI, the number of marrow cavities surrounded by bone, and the number of connections that must be broken to split the structure into two parts. A more convenient approach is to relate the connectivity to the total volume of VOI and express this parameter as connectivity density [19]. The Degree of Anisotropy describes the orientation of the structural elements in the bone. DA specifies whether the trabeculae have a particular orientation or are arranged randomly. The calculation is based on the mean intercept length from various directions [20].

3 Materials and Methods

3.1 Datasets Used

In this work, X-ray microCT data of 4-month-old pigs after LIF surgery were used. One-level LIF surgery was conducted on Lumbar 2 and Lumbar 3 (L2–L3) vertebrae. The samples were divided into three groups according to the material for LIF used. A bone autograft from the iliac crest was used in the first group (group A). In the second group (group B) was used a biodegradable nanocomposite implant of biphasic calcium phosphate [2] modified with collagen/oxycellulose biopolymeric foam, enriched with fibroblast growth factor 2 [21]. In the third group (group C), similarly composed biomaterial as in group B was used, but the fibroblast growth factor 2 was substituted by bioactive polyphosphate. All samples were after the LIF surgery fixed with the pedicle screws [22].

The fused vertebrae were surgically removed, wrapped into the plastic foil to avoid samples drying, and scanned on microCT system GE phoenix vltomelx L 240 (Waygate Technologies, USA). The voltage of the scan was 100 kV, the current was 300 μ A and the X-ray beam was filtered by a 1.5 mm aluminum filter. In total, 2200 projections were captured with the detector exposure time of 400 ms. For more about the samples and their measurement, see [14].

3.2 Determination of Volume of Interest

All datasets were firstly registered in the coordinate system according to the top-cranial and bottom-caudal orientation, where the L2 vertebra is located in the upper part of the volume. Consequently, a prepared surface mesh representing the LIF area was fitted on the sample using VG Studio MAX 3.4 (Volume Graphics GmbH, Germany). The manually pre-fitted mesh was consequently automatically registered using the best fit tool. The mesh fitted in the 3D volumetric data created the VOI. VOI was consequently extracted and further analyzed (see Fig. 1b).

Preparation of the mesh representing the LIF area was conducted by manual segmentation of the LIF area in 6 samples. Binary masks were consequently averaged and smoothed using a gaussian filter (see Fig. 1a). This procedure was conducted in Matlab (MathWorks, Inc).

3.3 Image Analysis

Evaluation of the newly formed bone in the LIF area is based on the quantification of seven parameters: Trabecular In Growth Ratio (TIGR) acquired from [14], mean

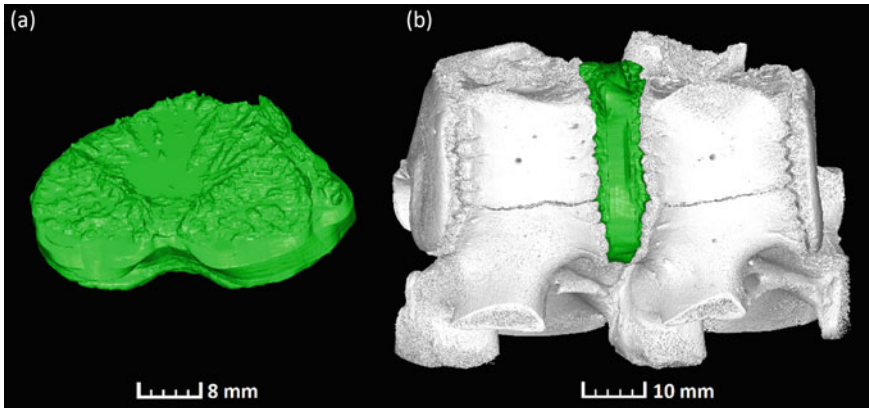


Fig. 1 **a** Surface mesh representing the LIF area. **b** Mesh registered into the sample in order to extract the LIF area for further evaluation

Tb.Th, mean Tb.Sp, BV/TV, Tb.N, Conn.D and DA. TIGR value represents the ratio between the fused area, and the area of facies intervertebralis.

Within a determined VOI was quantified a bone tissue volume (BV), using VG Studio MAX 3.4. The suggested threshold according to the image histogram for advanced surface determination was used. Since the mesh fitted into the LIF area of individual samples always has the same volume, the total volume (TV) used in the BV/TV parameter is determined in advance.

Extracted VOIs of each measured sample were processed in ImageJ software using the BoneJ plugin [23]. Three parameters were quantified by BoneJ: Tb.Th, connectivity, density, and anisotropy. Firstly, the samples were segmented to extract the bone volume. Segmentation proceeded using Otsu thresholding, according to [24]. Consequently, the binary mask was purified to remove all particles. Purification is based on the analysis of connected components and removes all particles surrounding the largest component. Such particles may have been formed by potential noise in the data. Lastly, Tb.Th, Conn.D, and DA were calculated using the BoneJ—see Tb.Th calculation in Fig. 2). Since the anisotropy calculation is a stochastic process, the calculation proceeded three times, and the mean value was chosen as a representative.

Tb.N and Tb.Sp were calculated according to the following equations: (Eqs. 1, 2 respectively):

$$\text{Tb.N} = (\text{BV}/\text{TV})/\text{Tb.Th} \tag{1}$$

$$\text{Tb.Sp} = (1/\text{Tb.N}) - \text{Tb.Th} \tag{2}$$

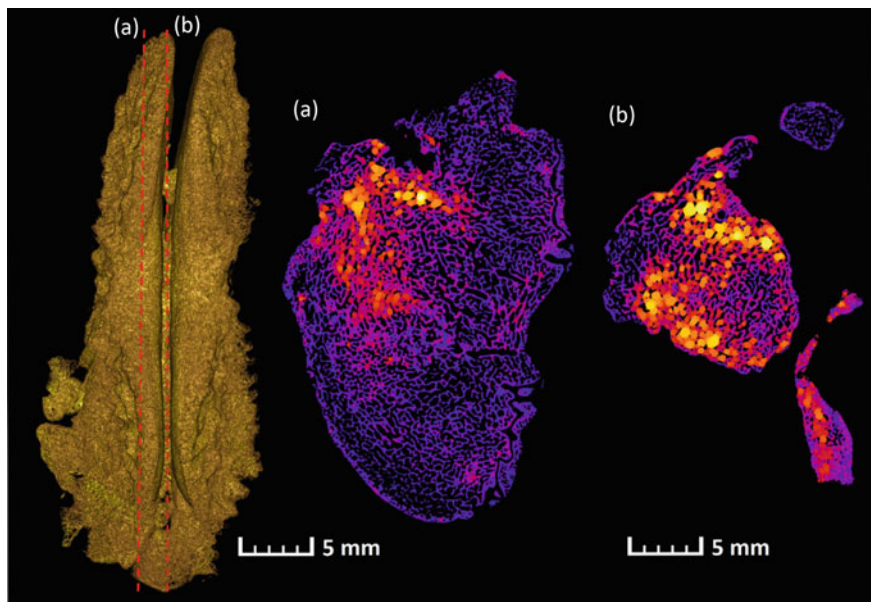


Fig. 2 Analysis of trabecular thickness. **a** Cross-section in the location of facies intervertebralis, **b** Cross-section in the area of LIF. Brighter color depicts larger trabeculae

4 Results

Evaluation of the newly formed bone is characterized by obtained parameters in Table 1. Samples are divided into three groups. Group A—bone graft, group B and C—different biomaterials (see Sect. 3.1). According to the TIGR¹ value, vertebrae fusion proceeded the best by the samples in group B, taking into account the average value. The standard deviation, on the contrary, is the highest because sample 2 in this group did not fuse at all. The TIGR value coincides with the mean Tb.Th value, which is also the highest in group B, and also has the highest standard deviation.

In the samples where the bone graft was used (group A), trabeculae formed with the greatest distance apart of all groups (mean Tb.Sp = 0.45), but the trabeculae had the highest value of connectivity density (4.14 mm^{-3}). The evaluation parameters in group C manifest the lowest amount of newly developed bone. This is given by insufficient osteogenesis function of the bioimplant used within this group. Especially the TIGR value and Conn.D parameters indicate the fusion fragility.

The parameters characterizing the morphometry of the newly formed bone do not manifest big differences among individual groups—see graph in Fig. 3. The largest percentage difference is in Tb.N, where group B has the highest amount of trabecular bone. This is related to the small Tb.Sp value in this group and thus the increased BV/TV value. On the contrary, the smallest difference is in the mean Tb.Th value.

¹ Trabecular in Growth Ratio (TIGR) acquired from [14].

Table 1 Morphometric parameters of analyzed bone tissue

	Sample	TIGR (%)	Mean Tb.Th (mm)	Tb.Sp (mm)	BV/TV	Tb.N (1/mm)	Conn.D (mm ⁻³)	DA (-)
Group A	1	1.6	0.27	1.06	0.20	0.75	2.96	0.38
	2	7.1	0.23	0.25	0.48	2.08	5.17	0.16
	3	4.8	0.28	0.42	0.40	1.42	3.77	0.22
	4	3.6	0.23	0.26	0.46	2.04	3.65	0.20
	5	22.7	0.25	0.24	0.52	2.02	5.16	0.10
	Average	8.0	0.25	0.45	0.41	1.66	4.14	0.21
Group B	1	16.3	0.23	0.19	0.55	2.38	3.95	0.21
	2	0.0	0.43	0.53	0.45	1.04	1.37	0.25
	3	1.5	0.20	0.21	0.48	2.43	4.55	0.19
	4	29.8	0.31	0.17	0.64	2.10	2.99	0.23
	5	28.8	0.21	0.28	0.42	2.03	2.78	0.15
	Average	15.3	0.28	0.28	0.51	2.00	3.13	0.21
Group C	1	0.2	0.27	0.33	0.46	1.66	2.91	0.31
	2	4.7	0.27	0.36	0.42	1.59	2.71	0.11
	3	2.2	0.26	0.31	0.46	1.76	2.75	0.16
	4	3.1	0.20	0.33	0.38	1.86	3.40	0.10
	5	4.0	0.32	0.38	0.45	1.43	2.57	0.15
	Average	2.8	0.26	0.34	0.43	1.66	2.87	0.17

This fact can indicate that the trabeculae have the same thickness within all groups and do not affect the quality of intervertebral fusion.

5 Newly Formed Bone Evaluation

It is interesting to look into the relationship between the TIGR value representing the amount of the fused area and morphometric parameters describing the bone properties. There is evident a linear relationship between the TIGR value and Tb.N and Conn.D, respectively. Increasing the fused bone ratio (the TIGR value) also increases the number of trabeculae and their connectivity density. It means that the bone in the LIF area expands as a connected unit. Bone expansion takes place so that the newly formed bone attaches to both vertebrae (in high TIGR values). If the newly formed bone were attached only to one vertebra, the TIGR value would be small (Fig. 4).

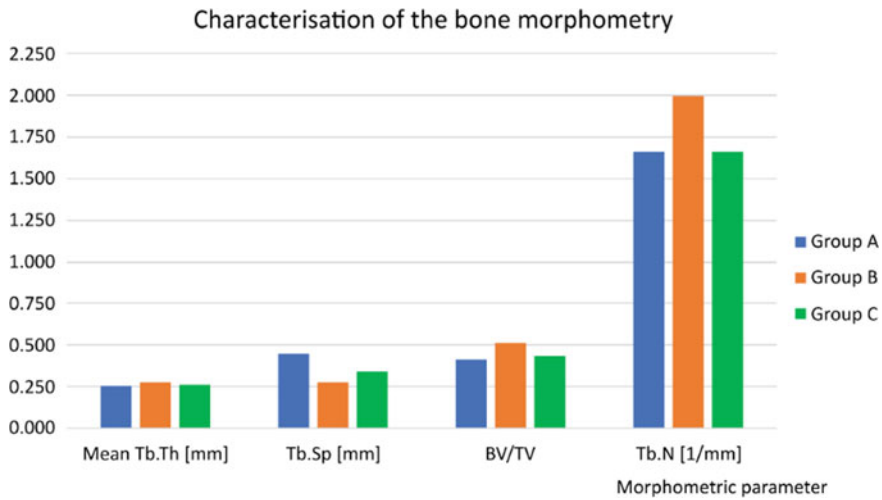


Fig. 3 Graph comparing selected morphological parameters of newly formed bone in the location of LIF area. Individual color bars represent individual groups of samples

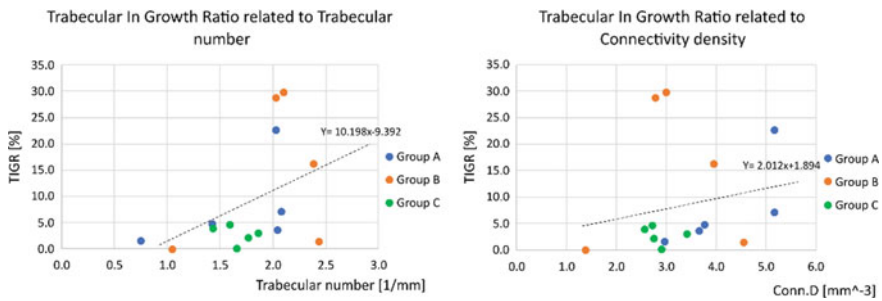


Fig. 4 Graphs depicting the relationship between the ratio of the fused bone (*TIGR* trabecular in growth ratio) and the trabecular number, connectivity density respectively

6 Conclusion and Future Work

In this paper, we proposed a methodology to automatically characterize the morphometry of the bone in the fused region after the LIF surgery. The study was elaborated using the samples of porcine vertebrae, where the LIF was conducted using three different types of implants. The main benefit of the proposed methodology is an automatic 3D approach for the evaluation of bone tissue. Automated characterization of fused bone is suitable for accurate comparison of samples where vertebrae are fused with different types of intervertebral implants. The analysis is not affected by operator-induced inaccuracies and is therefore suitable for the inter-laboratory evaluation of osteogenesis bioimplant function in preclinical studies.

In the future, we would like to extend this methodology to the processing of human fused vertebrae samples. Using clinical CT images cannot provide all information mandatory for the analyses described in this paper, but we would utilize the methodology for LIF area extraction and quantify different parameters, such as bone mineral density, bone volume, and detection of fractures or abnormalities in the newly formed bone. The utilization of CT is a standardized diagnostics tool in the pre- and post-surgery diagnosis of LIF. An automated approach for assessing the structure of bone formation between vertebrae may expand the possibilities of diagnosing the success of LIF surgery.

Acknowledgements Grant CEITEC VUT-K-22-7761 is realised within the project Quality Internal Grants of BUT (KInG BUT), Reg. No. CZ.02.2.69/0.0/0.0/19_073/0016948, which is financed from the OP RDE.

References

1. Fujibayashi, S., et al.: A novel synthetic material for spinal fusion: a prospective clinical trial of porous bioactive titanium metal for lumbar interbody fusion. *European Spine Journal*, 20(9), 1486–1495 (2011), <https://doi.org/https://doi.org/10.1007/s00586-011-1728-3>.
2. Stastny, P., et al.: Structure degradation and strength changes of sintered calcium phosphate bone scaffolds with different phase structures during simulated biodegradation in vitro. *Materials Science and Engineering: C*, 100, 544–553 (2019), <https://doi.org/https://doi.org/10.1016/j.msec.2019.03.027>.
3. Chen, L., et al.: Lumbar interbody fusion with porous biphasic calcium phosphate enhanced by recombinant bone morphogenetic protein-2/silk fibroin sustained-released microsphere: an experimental study on sheep model. *Journal of Materials Science: Materials in Medicine*, 26(3), (2015), <https://doi.org/10.1007/s10856-015-5463-x>.
4. Lo, W.-C., et al.: Understanding the Future Prospects of Synergizing Minimally Invasive Transforaminal Lumbar Interbody Fusion Surgery with Ceramics and Regenerative Cellular Therapies. *International Journal of Molecular Sciences*, 22(7), (2021), <https://doi.org/10.3390/ijms22073638>.
5. Schmidt, C., et al.: Precision and Accuracy of Peripheral Quantitative Computed Tomography (pQCT) in the Mouse Skeleton Compared With Histology and Microcomputed Tomography (μ CT). *Journal of Bone and Mineral Research*, 18(8), 1486–1496 (2003), <https://doi.org/10.1359/jbmr.2003.18.8.1486>.
6. He, T., et al.: A comparison of micro-CT and histomorphometry for evaluation of osseointegration of PEO-coated titanium implants in a rat model. *Scientific Reports*, 7(1), (2017), <https://doi.org/10.1038/s41598-017-16465-4>.
7. Lyu, H.-Z., et al.: Correlation between two-dimensional micro-CT and histomorphometry for assessment of the implant osseointegration in rabbit tibia model. *Biomaterials Research*, 25(1), (2021), <https://doi.org/10.1186/s40824-021-00213-x>.
8. Kitchen, D., et al.: Fusion Assessment by MRI in Comparison With CT in Anterior Lumbar Interbody Fusion: A Prospective Study. *Global Spine Journal*, 8(6), 586–592 (2018), <https://doi.org/https://doi.org/10.1177/2192568218757483>.
9. Sethi, A., et al.: Radiographic and CT Evaluation of Recombinant Human Bone Morphogenetic Protein-2-Assisted Spinal Interbody Fusion. *American Journal of Roentgenology*, 197(1), 128–133 (2011), <https://doi.org/https://doi.org/10.2214/AJR.10.5484>.

10. Brans, B., et al.: Assessment of bone graft incorporation by 18 F-fluoride positron-emission tomography/computed tomography in patients with persisting symptoms after posterior lumbar interbody fusion. *EJNMMI Research*, 2(1), (2012), <https://doi.org/10.1186/2191-219X-2-42>.
11. Gadomski, B. et al.: Evaluation of lumbar spinal fusion utilizing recombinant human platelet derived growth factor-B chain homodimer (rhPDGF-BB) combined with a bovine collagen/ β -tricalcium phosphate (β -TCP) matrix in an ovine model. *JOR SPINE*, 4(3), (2021), <https://doi.org/10.1002/jsp2.1166>.
12. Tan, G. H., et al.: CT-based classification of long spinal allograft fusion. *European Spine Journal*, 16(11), 1875–1881 (2007), <https://doi.org/https://doi.org/10.1007/s00586-007-0376-0>.
13. Bridwell, K. H., et al.: Anterior Fresh Frozen Structural Allografts in the Thoracic and Lumbar Spine. *Spine*, 20(12), 1410–1418 (1995), <https://doi.org/https://doi.org/10.1097/00007632-199506020-00014>.
14. Laznovsky, J., et al.: Automatic 3D analysis of the ex-vivo porcine lumbar interbody fusion based on X-ray micro computed tomography data. *Computers in Biology and Medicine* 145, (2022), <https://doi.org/10.1016/j.compbiomed.2022.105438>.
15. Gupta, A., et al.: Bone graft substitutes for spine fusion: A brief review. *World Journal of Orthopedics*, 6(6), (2015), <https://doi.org/10.5312/wjo.v6.i6.449>.
16. Jiang, Y., et al.: Application of micro-ct assessment of 3-d bone microstructure in preclinical and clinical studies. *Journal of Bone and Mineral Metabolism*, 23(S1), 122–131 (2005), <https://doi.org/https://doi.org/10.1007/BF03026336>.
17. Boerckel, J. D., et al.: Microcomputed tomography: approaches and applications in bioengineering, 5(6), (2014), <https://doi.org/10.1186/scri534>.
18. Bouxsein, M. L., et al.: Guidelines for assessment of bone microstructure in rodents using micro-computed tomography. *Journal of Bone and Mineral Research*, 25(7), 1468–1486 (2010), <https://doi.org/https://doi.org/10.1002/jbmr.141>.
19. Odgaard, A., Gundersen, H. J. G Quantification of connectivity in cancellous bone, with special emphasis on 3-D reconstructions. *Bone*, 14(2), 173–182 (1993), [https://doi.org/https://doi.org/10.1016/8756-3282\(93\)90245-6](https://doi.org/https://doi.org/10.1016/8756-3282(93)90245-6).
20. Odgaard, A. Three-dimensional methods for quantification of cancellous bone architecture. *Bone*, 20(4), 315–328 (1997), [https://doi.org/https://doi.org/10.1016/S8756-3282\(97\)00007-0](https://doi.org/https://doi.org/10.1016/S8756-3282(97)00007-0).
21. Vojtova, L., et al.: Healing and Angiogenic Properties of Collagen/Chitosan Scaffolds Enriched with Hyperstable FGF2-STAB® Protein: In Vitro, Ex Ovo and In Vivo Comprehensive Evaluation. *Biomedicines*, 9(6), (2021), <https://doi.org/10.3390/biomedicines9060590>.
22. Krticka, M., et al.: Lumbar Interbody Fusion Conducted on a Porcine Model with a Biore-sorbable Ceramic/Biopolymer Hybrid Implant Enriched with Hyperstable Fibroblast Growth Factor 2. *Biomedicines*, 9(7), (2021), <https://doi.org/10.3390/biomedicines9070733>.
23. Domander, R., et al.: BoneJ2 - refactoring established research software. *Wellcome Open Research*, 6, (2021), <https://doi.org/10.12688/wellcomeopenres.16619.2>.
24. Parkinson, I. H., et al.: Variation in segmentation of bone from micro-CT imaging: implications for quantitative morphometric analysis, 31(2), 160–164 (2008), <https://doi.org/https://doi.org/10.1007/BF03178592>.